We are IntechOpen, the world's leading publisher of Open Access books Built by scientists, for scientists

6,900
Open access books available

185,000
International authors and editors

200M
Downloads

Our authors are among the

154
Countries delivered to

TOP 1%
most cited scientists

12.2%
Contributors from top 500 universities



WEB OF SCIENCE™

Selection of our books indexed in the Book Citation Index in Web of Science™ Core Collection (BKCI)

Interested in publishing with us?
Contact book.department@intechopen.com

Numbers displayed above are based on latest data collected.
For more information visit www.intechopen.com



Chapter 6

Super-Lubricious, Fullerene-like, Hydrogenated Carbon Films

Bin Zhang, Kaixiong Gao, Yuanlie Yu and Junyan Zhang

Additional information is available at the end of the chapter

http://dx.doi.org/10.5772/intechopen.70412

Abstract

Almost one-third of minimal energy is consumed via friction and wear process. Thus, to save energy using advanced lubrication materials is one of the main routes that tribologists are focused on. Recently, superlubricity is the most prominent way to face energy problems. Designing promising mechanical systems with ultra-low friction performance and establishing superlubricity regime is imperative not only to the most greatly save energy but also to reduce hazardous waste emissions into our environment. At the macroscale, hydrogenated diamond-like carbon (DLC) film with a supersmooth and fully hydrogen terminated surface is the most promising materials to realize superlubricity. However, the exact superlubricity of DLC film can only be observed under high vacuum or specific conditions and is not realized under ambient conditions for engineering applications. The latest breakthrough in macroscale superlubricity is made by introducing fullerene-like nano-structure and designing graphene nanoscroll formation, which also demonstrates the structure-superlubricity (coefficient of friction ~0.002) relationship. Thus, it is very interesting to design macroscale superlubricity by prompting the in situ formation of these structures at the friction interfaces. In this chapter, we will focus on fullerene-like hydrogenated carbon (FL-C:H) films and cover the growth methods, nanostructures, mechanic, friction properties and superlubricity mechanism.

Keywords: fullerene-like, carbon films, superlubricity, friction

1. Introduction

People have a love and hate relationship with friction because we need high friction some times (like braking) but we expect the friction to be as small as possible in the machines which might help to save energy. The energy issue pushes us to develop more robust lubricious

IntechOpen

© 2018 The Author(s). Licensee IntechOpen. This chapter is distributed under the terms of the Creative Commons Attribution License (http://creativecommons.org/licenses/by/3.0), which permits unrestricted use, distribution, and reproduction in any medium, provided the original work is properly cited. CC BY

materials. Nowadays, superlubricity is a most fascinating word not only in mind but also in practice [1–5]. Designing promising mechanical systems with ultra-low friction performance and establishing superlubricity regime is imperative not only to the most greatly save energy but also to reduce hazardous waste emissions.

Motivated by these issues, superlubricity has aroused extensive attention of many research groups and therefore an active topic in many fields [6–11]. Not surprisingly, superlubricity has been realized in some experiments associated with layered materials such as graphene, molybdenum disulphide (MoS_2), highly oriented pyrolytic graphite (HOPG) and multi-walled carbon nanotubes (MWCNT) [6, 12–15]. At the macroscale, hydrogenated diamond-like carbon (DLC) film with a supersmooth and fully hydrogen-terminated surface is the most promising material to realize superlubricity [4, 16]. However, the exact superlubricity of DLC film can only be observed under high vacuum or specific conditions and is not realized under ambient conditions for engineering applications [17]. The latest breakthrough in macroscale superlubricity is made by introducing fullerene-like nano-structure and designing graphene nanoscroll formation, which also demonstrates the structure-superlubricity (coefficient of friction ~0.002) relationship [5, 18].

In general, lubricating materials satisfying engineering application face some problems such as macro contact area (≥ mm × mm), withstanding high contact pressure (≥1 GPa) and exposure to air environment (H_2O, O_2, etc.), which are more prominent problems for designing and realizing macroscale superlubricity [19–24]. But, luckily, Zhang et al. fabricated fullerene-like hydrogenated carbon (FL-C:H) films and achieved superlubricity under engineering conditions [5, 18, 24–28]. The curvature structure of fullerene-like structure extends the strength of graphite plane hexagon into three dimension space network, in turn, increasing the hardness and elasticity of carbon films, demonstrating super low friction in air, meaning solid superlubricity with engineering application value [18, 26]. Most interestingly, the fullerene-like structure of the carbon films could be adjusted via the hydrogen content, bias supply, in the deposition gas sources [29–33]. Thus, it is very interesting to design macroscale superlubricity by prompting the in situ formation of these structures at the friction interfaces.

Usually, both plasma-enhanced chemical vapor deposition (PECVD) and reactive magnetron sputtering can be employed to growth FL-C:H films which one can find in early reports [5, 27]. When using PECVD, the pulse power and the reasonable atmosphere are necessary. FL-C:H films are growing in miexed atmosphere of CH_4 and H_2 with flow ratio at 1:2, but the deposition pressure can adjust from 10 to 20 Pa depending on different chambers [5, 34]. But for reactive magnetron sputtering, distinction from PECVD are that the additional magnetic field and no H_2 anymore [21, 27]. The most important thing when using reactive magnetron sputtering is that a deep poisoning mode is employed [27, 28]. So, as we see, deep poisoning reactive magnetron sputtering can also be mentioned as magnetic field assistant PECVD. Such difference might influence the growth mechanisms which we will discuss later.

2. Structural characterizations

As one known, carbon-based curve structure is variety of things, such as carbon nanotubes, fullerenes, carbon nitride nanotubes and so on [35, 36]. FL-C:H films and its structures are

http://dx.doi.org/10.5772/intechopen.70412

very similar to fullerene-like carbon nitride (FL-CNx) films [37], within distorted multi-storey multilayer graphene intersecting and interlocked in an amorphous carbon matrix, show high hardness, high elastic recovery and high resistance to deformation. A typical high resolution transmission electron images (HRTEM) of FL-C:H films, grown via high impulse power (which is usually employed in magnetron sputtering, mentioned as high power impulse magnetron sputtering (HiPIMS) [26]) assistant PECVD, displays in **Figure 1a**. Atomic force acoustic microscope (AFM) imaging (**Figure 1b**) under tapping mode was used to inspect the cluster domains in the films and indicate that the film has a special nanocomposite structure with graphene domains dispersed in an amorphous carbon matrix [26].

These special nanostructures can also be inspected by Raman spectrum. Usually, FL-C:H films exhibit typical character of diamond-like carbon films in the region of 1000–2000 cm^{-1}, but with some additional peaks at about 400 and 700 cm^{-1} and a distinct shoulder at around 1230 cm^{-1} **(Figure 2a)** [34]. The two low intermediate wave number bands near 400 cm^{-1} and 700 cm^{-1} are very similar to that of fullerene-like carbon nitride that can be assigned to relaxation of Raman selection rule due to the curvature in graphene planes, which appears to induce Raman scattering away from the G point [38]. The same bands are also present in the Raman spectra acquired from carbon onions and C_{60} that have been attributed to the transverse optic and transverse acoustic vibrations at the M point [38]. Thus, an acceptable fitting could only be reached via four Gaussian peaks at about 1230, 1350, 1470, and 1560 cm^{-1}, respectively **(Figure 2b)** [9, 27, 28, 34]. Thus, we can consider that all peaks at around 400, 700, 1230 and 1480 cm^{-1} are all active from that of fullerene-like structure with curled graphene planes.

Thanks to the adjustable conditions and methods, the nanostructures of FL-C:H films can be tailored as one expecting. In fact, either a conventional PECVD or a magnetic field assistant

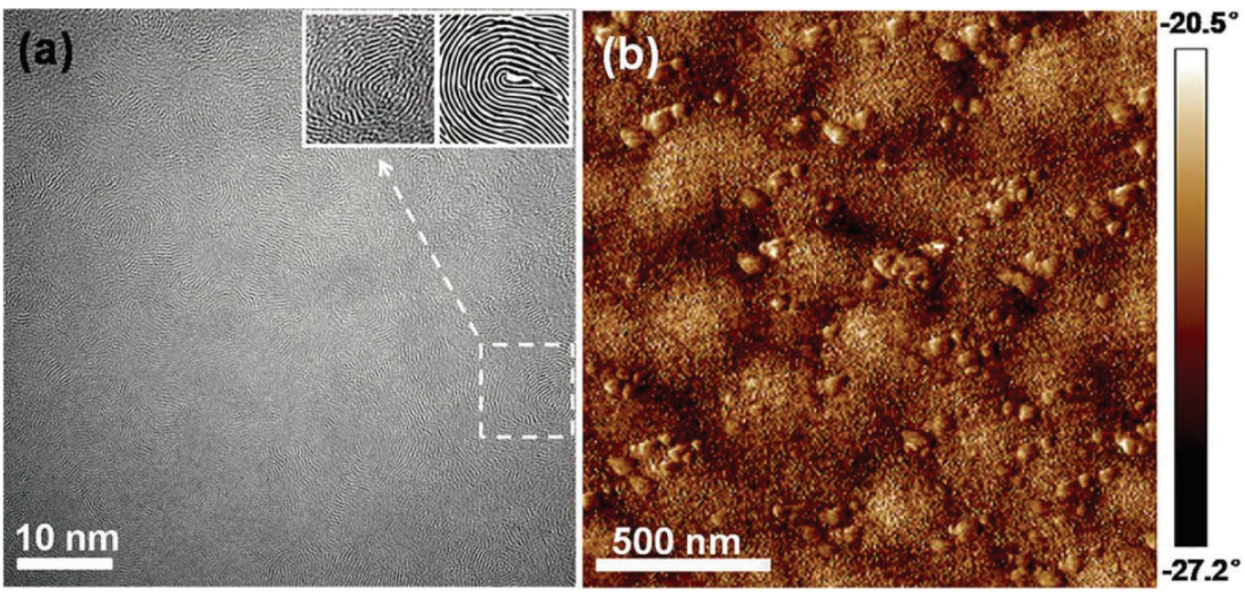


Figure 1. (a) High resolution transmission electron images of the FL-C:H films. Insets: carbon fingerprint and human fingerprint pattern. (b) An AFM phase image of the FL-C:H films deposited on silicon wafers. (Reproduced from Ref. [26] with permission from the Royal Society of Chemistry).

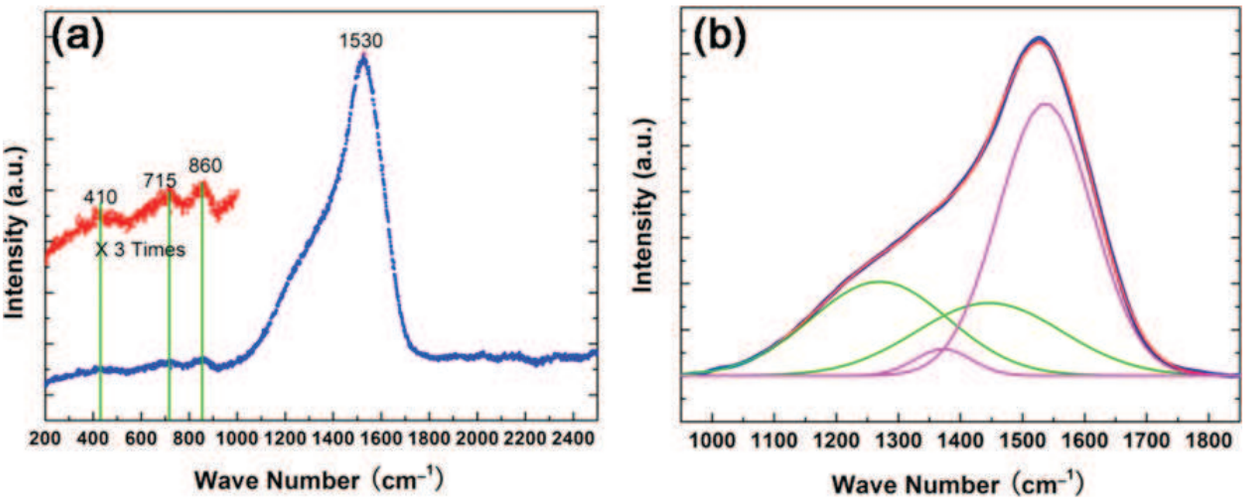


Figure 2. Raman spectra of hydrogenated carbon film deposited by dc-pulse plasma CVD. (a) Raman spectrum and magnified wave number region from 0 to 1000 cm^{-1} and (b) deconvoluted wave number region from 1000 to 2000 cm^{-1} in the Raman spectrum of (a).

PECVD (reactive magnetron sputtering), an important thing is that bias voltage has a main effects on nanostructures. Though the outfield auxiliary in reactive magnetron sputtering lowers the growth pressure directly, both high voltage and low duty cycle are crucial. During reactive magnetron sputtering process [21], the prominent FL-C:H films grown at −800 V bias exhibit the highest hardness of 20.9 GPa as well as elastic recovery of about 85%. The further increase of bias voltage cripples the mechanical due to further graphitization of the films. But very different nanostructure can be observed under low bias of −100 V, which is called amorphous carbon films dispersed with multilayer graphenes. It is very different from the films grown via PECVD that one can seen that with increasing the bias voltage, the hardness decreases while the elastic recovery keeps increasing [39]. The probable reason is that, at low pressure with the outfield auxiliary in reactive magnetron sputtering process, ions have higher free energy than that in PECVD which might induce easier graphitization.

On the other hand, the pulse duty cycles determine the local relaxation of the distorted chemical bonds. According to the typical subplantation model suggested by Robertson [40], three scales during ion interaction with the film are addressed that: the cascade, 10^{-14} s; the thermal spike, 10^{-12} s; and the longer time relaxation, ~10^{-9} s. The longer time relaxation time benefits the stress releasing and hydrogen removing which contributes to restructuring of carbon matrix. In our work, the annealing time is almost ~10^{-5} s, far than ~10^{-9} s, thus, the depositing pulse film has a completely surface, thereby restricting the formation of pentagonal rings which are associated with the ion bombardment at the pulse-on/off state [41]. As shown in **Figure 3**, one can see that with the pulse-on time increases while pulse-off time decrease, more curved graphene structures are arisen. These variations are also confirmed by Raman spectra, showing in **Figure 4**. With decrease in duty cycles, a shoulder at around 1230 cm^{-1} comes more obviously, which is believed from that of fullerene-like structure with curled graphene planes, in accordance well with HRTEM results. Here, Raman spectra of these films are simulated using four vibrational bands at 1260, 1380, 1470, and 1570 cm^{-1} [9, 27, 29, 34], respectively (**Figure 4**), these with A-type symmetry (from five-, six-, and seven-membered

http://dx.doi.org/10.5772/intechopen.70412

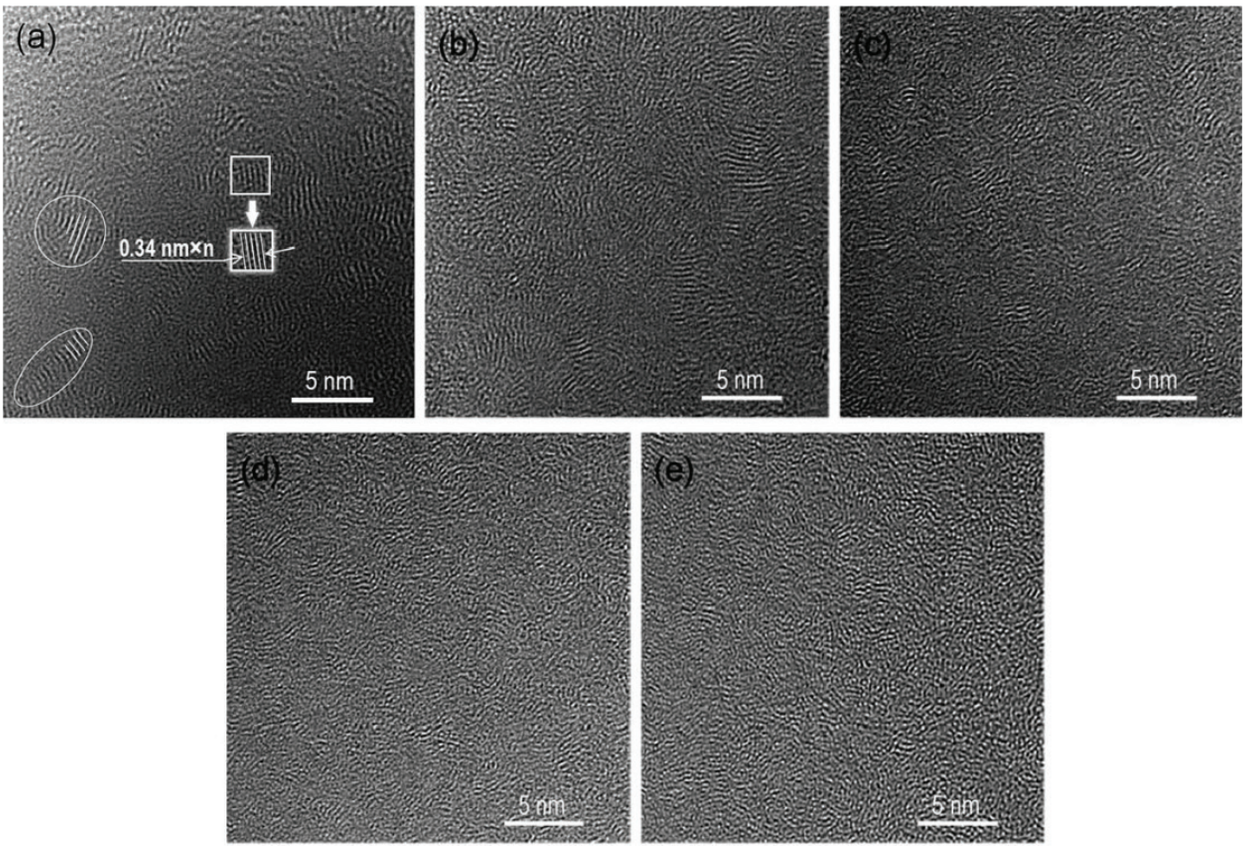


Figure 3. HRTEM images of the as-prepared films with pulse duty cycles of (a) 100%, (b) 80%, (c) 60%, (d) 40%, and (e) 20%. (Reproduced from Ref. [42] with permission from the Royal Society of Chemistry).

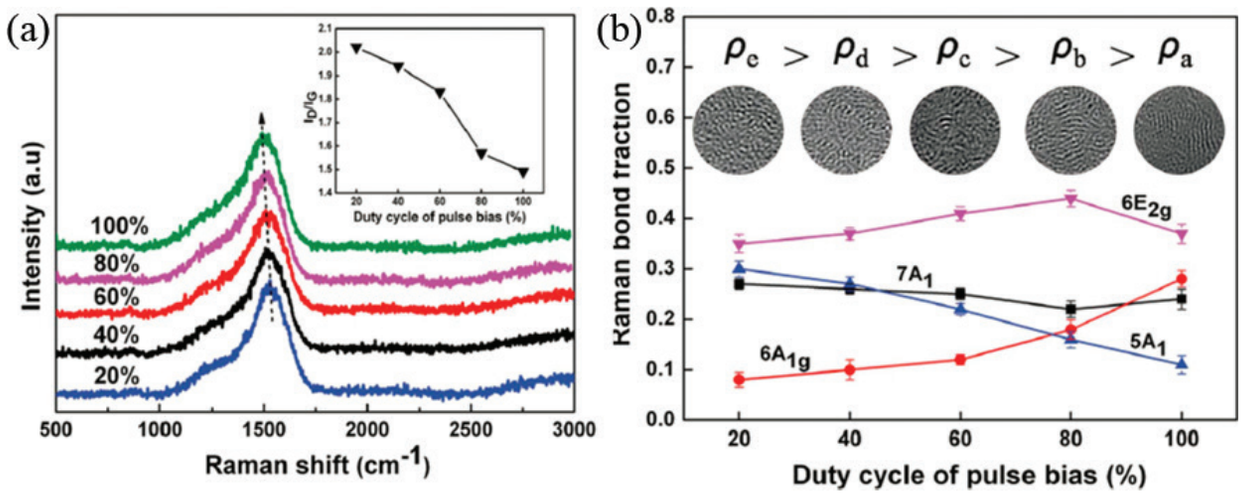


Figure 4. (a) Raman spectra of the as-prepared films at different pulse bias duty cycle. (b) Contribution to the carbon Raman band from the vibrations of five-, six- and seven-member rings versus the pulse duty cycle. (Reproduced from Ref. [42] with permission from the Royal Society of Chemistry).

rings) and one with E-type symmetry (from six-membered rings). The results show that even member rings and odd member rings have an opposite trend, and high odd member rings indicate the decrease and more fullerene-like structure.

Atmosphere influence on the nanostructures of FL-C:H films have been studied widely. Heterogeneous gases, such as H_2 and CF_4, introducing in growth process have different effects [29–33]. Interestingly, the growth of FL-C:H films show a conflicting to Hellgren's work [43] that intentional hydrogen addition to the discharge will terminate potential bonding sites for CNx precursors and hinder the growth of fullerene-like structures. But it seem that during growth FL-C:H films, hydrogen atoms during the deposition process may affect the production of odd rings by two competing ways: (1) stress induced by H^+ leads to the introduction of odd ring into flat graphene plane; (2) H^+ preferentially etches the plane's sp^2 phase and destroys the bond basis if forming odd rings. But more H_2 existing in growth condition has no much help on growing fullerene-like structures, so the effects of hydrogen need to be studied in detail. However, CF_4 show different influence on the nanostructures of the FL-C:H films. At low fluorine content, many C sites bond to neighboring C and the films microstructure displays lots of well organized graphite-like and fullerene-like fragments. But as the amount of F incorporated in the network increase, F-terminated large rings, Branches and chains with sp^2 sites densify and start to interact with each other and features like interlocking pore and amorphousness strongly prevail in the nanostructure [30, 32].

3. Mechanical and tribology properties

As we know, thanks to the unique topological structure, fullerene, predicted by Ruoff [44], have higher hardness than diamond, and have confirmed by other groups(is C60 fullerite harder than diamond). Vadim V. Brazhkin has synthesized a new nanomaterial by high-temperature treatment of fullerite C60 at moderate (0.1–1.5 GPa) pressures attainable for large-volume pressure apparatus, which show a high (90%) elastic recovery and fairly hardness of about 10–15 GPa [45]. It is noteworthy that in our works, so-called FL-C:H films with curved graphenes show a elastic recovery (≥80) with hardness variation from 10 to 30 GPa, depending on the growth conditions. **Figure 5** shows typical load-displacement curve and friction coefficients as function of time. A superlubricity phenomenal is observed at load of 20 N with friction coefficient at 0.009. One can notice the elastic recovery value variation with the annealing temperatures and shows the highest recovery value as shown in **Figure 6**. It is easily understood if one employs pentatomic-heptatomic theory of Raman [27, 28]. At 300°C, films show the maximum of odd rings which indicates that the most value of curved graphene exiting inside the carbon amorphous matrix.

As discussed above, it is obvious that elastic recovery and friction properties are correlated with inner nanostructures of FL-C:H films. To confirm this, we also studied the elastic recovery and friction properties using the films growth under different duty cycles and H_2 flow rates. As we have already confirmed that lower duty cycle means more fullerene-like structure due to the long relaxing time. So the lower duty cycle declares that lower growth rate of the films thickness (**Figure 7** inset). One can also confirm that the hardness and the elastic recovery decrease with the decay of fullerene-like structure, as the decrease of odd member rings (**Figure 6**).

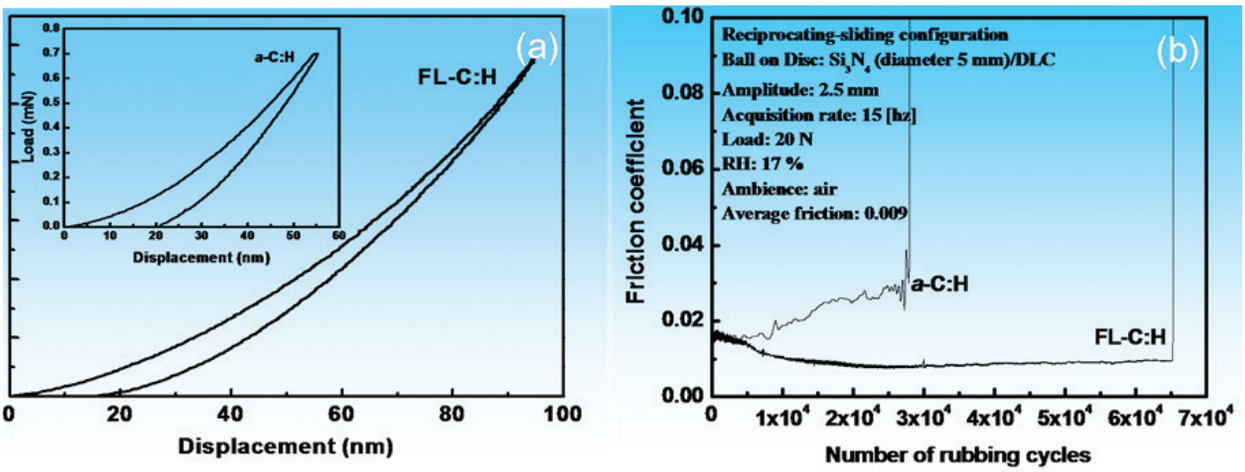


Figure 5. Typical load-displacement curve for the 1500 nm thick FL-C:H film annealed at 300°C, the inset is the load-displacement curve of 500 nm thick typical hydrogenated carbon films (a-C:H) (a) and tribological tests on the FL-C:H film in air with 20% relative humidity at ambient temperature (b).

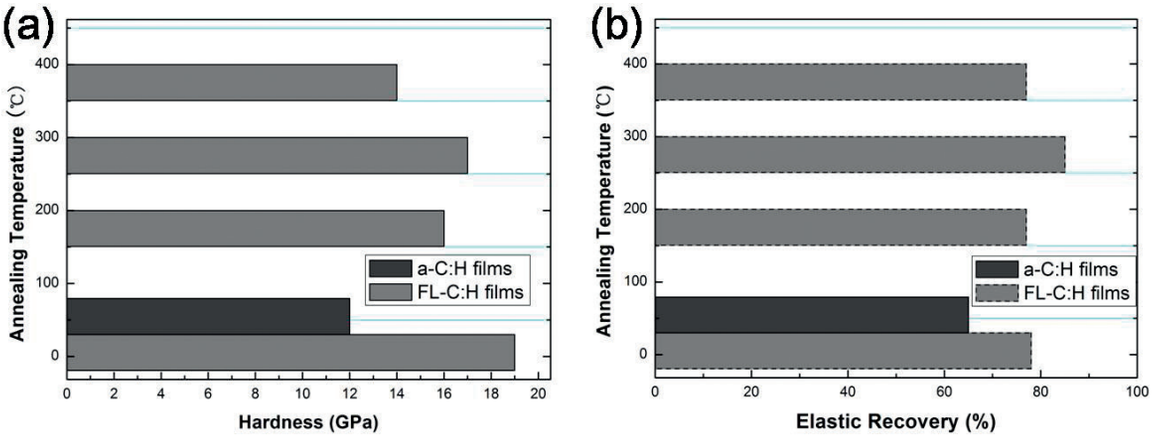


Figure 6. Mechanical properties of the FL-C:H film before and after annealing: (a) Hardness, and (b) Elastic Recovery. (All films were annealed for 1h in Ar at temperature of 200, 300 and 400°C, respectively).

Different from the single-way variation of the influence of duty cycle, the change of mechanical properties has a yielding point. As shown in **Figure 8**, the FL-C:H film grown at H_2 flow rate 5 SCCM show the lowest friction coefficient. Raman spectrum is employed here to quantify the odd member rings from both films and corresponding debris. It is showing that the friction coefficient has a significantly positive relation with odd member rings. That is, odd member rings confirm more fullerene-like structures which in turn, determine the hardness and tribology. So there is no excuse that fullerene-like structures contribute to mechanical and tribology properties.

To reveal how such structure affects on the tribology properties, X-ray diffraction (XRD) analysis has been performed at the original surface and wear debris and tracks of the FL-C:H films. The film pattern shows three peaks at about $2\theta = 69.1°$, 33° and 22.4°. The two peaks at $2\theta = 69.1°$ and 33° are from the silicon substrate ([004] and [002], respectively (**Figure 9**)). A

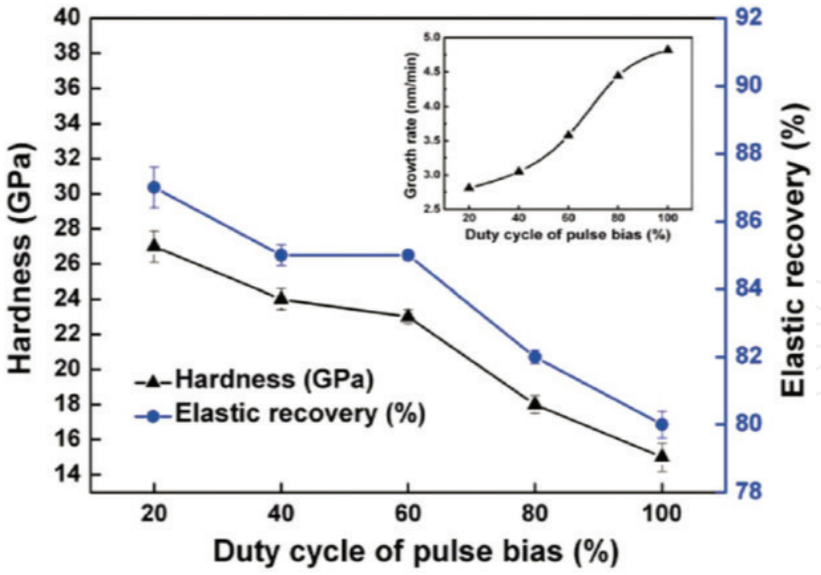


Figure 7. Hardness and elastic recovery of the as-prepared films with different pulse duty cycles. Inset show the growth rate of the as-prepared films with different pulse duty cycles. (Reproduced from Ref. [42] with permission from the Royal Society of Chemistry).

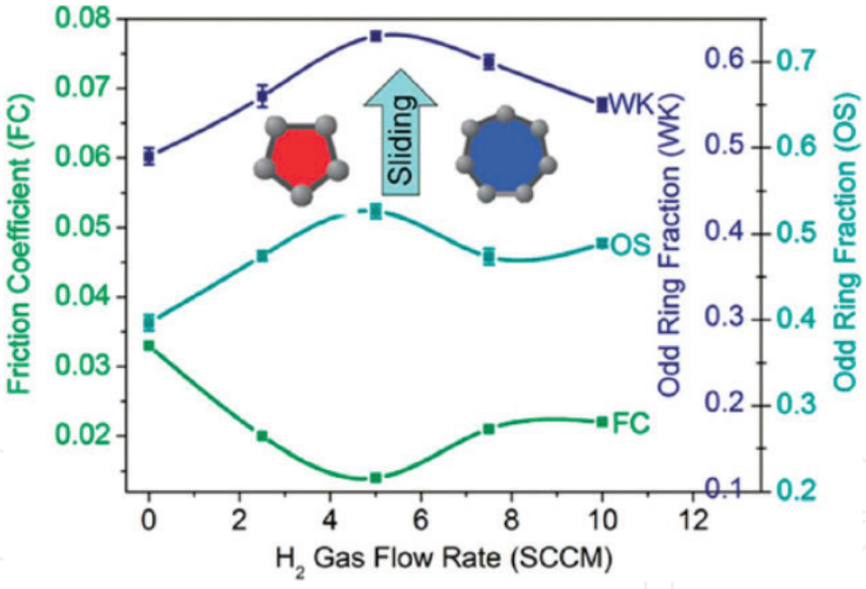


Figure 8. Friction coefficient and odd ring fraction of the FL-C:H films as a function of the gas flow rate of H_2. All the central wear tracks (WK) have a higher odd (pentagonal and heptagonal) carbon ring fraction than that of the originally deposited surfaces (OS). (Reproduced from Ref. [45] with permission from the Royal Society of Chemistry).

weak peak at $2\theta = 22.4°$, according with other studies [46], can be attributed to fullerene-like or onion-like nanoparticles (considering HRTEM and Raman results). And after friction testing, the peak at $2\theta = 22.4°$ become prominent, accompanying with a new band at $2\theta = 15°$ which arise from fullerene-like or onion-like nanoparticles, which leads low friction and small wear in open wear.

http://dx.doi.org/10.5772/intechopen.70412

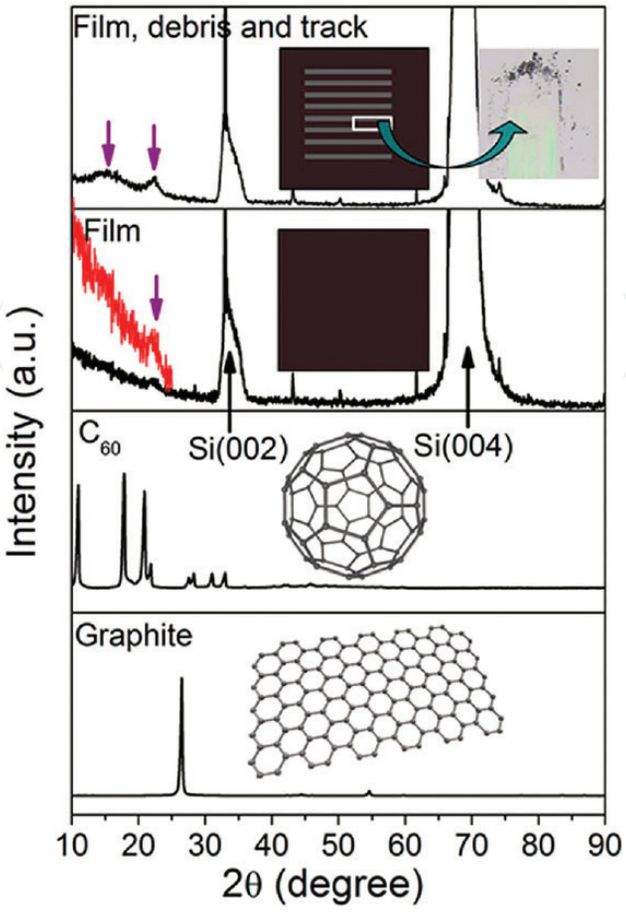


Figure 9. Experiment XRD patterns from the film and wear debris showing that the debris has a structure analogous to that of C60, far from that of nc-graphite. (Reproduced from Ref. [45] with permission from the Royal Society of Chemistry).

Besides, the affects of F incorporation, the humidity, variation of load, plasma process, etc., on the tribology properties of FL-C:H films were widely studied [21, 23–27]. Unfortunately, though the introducing of F atoms in carbon matrix is active hydrophobicity properties, and destroys the fullerene-like structures via terminating [30–32]. But humidity has a great influence on friction coefficients that, with increasing the humidity, the friction coefficient increases quickly to 0.08 at 50% for humidity. HRTEM results show that the onion-like nanoparticles in the debris are restrained: from spherical shell structure below 30% humidity to short curved graphene dispersed in amorphous matrix [26].

4. Superlubricity mechanisms

Benefit from unique bulk structures of FL-C:H films, some of well shelled graphene assemble nanoparticles are discovered on the friction interface. Thus, one can speculate that the main reason to the superlubricity is based on the bulk of fullerene-like structure which provides the

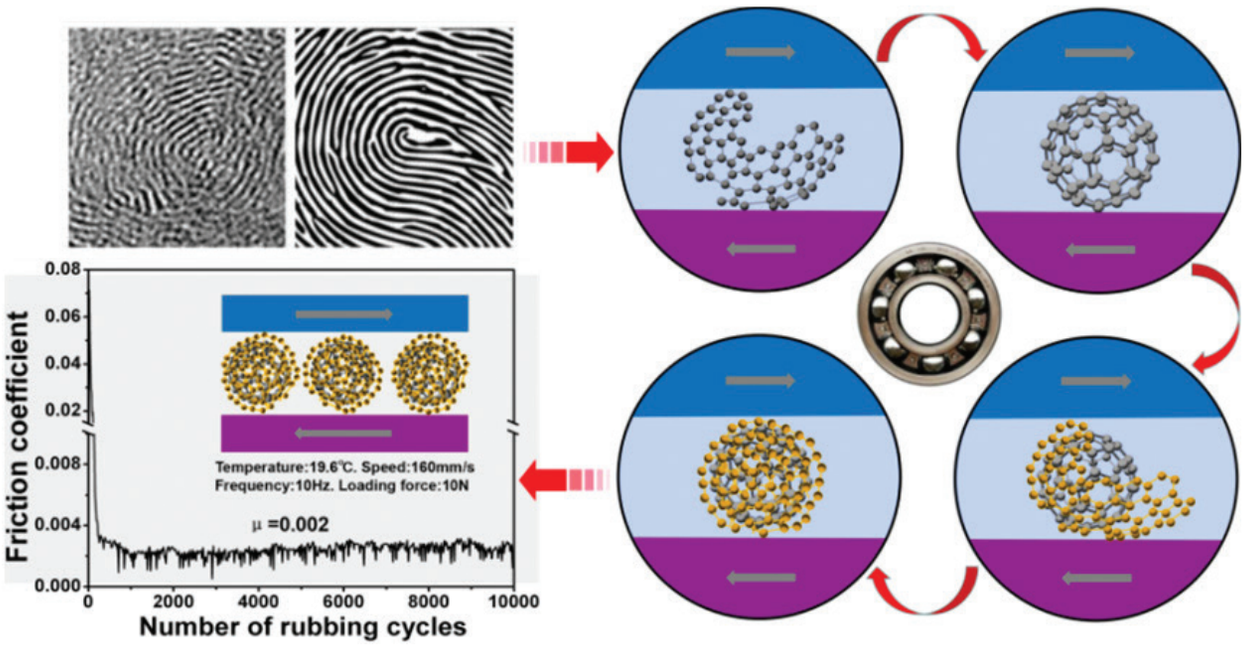


Figure 10. A incommensurate and rolling contact for the superlubricity of FL-C:H films. (Reproduced from Ref. [26] with permission from the Royal Society of Chemistry).

raw materials to grow of onion-like nanoparticles at certain conditions. One of issues worth exploring is that the onion-like nanoparticles only can see below 30% humidity. Theoretical model of the graphene to fullerene transformation confirmed that the formation of defects at the edge of graphene is the crucial step. Usually, water molecules exhibit higher activation energies that those of the non-polar adsorbates (O_2, N_2 and Ar) via stronger hydrogen bonds. Thus, at lower humidity, unsaturated dangling bonds of graphene have a high reaction activity and the hybridization are easy to occur on the edge of graphene itself, but at higher humidity, dangling bonds are saturated by water molecules, hindering the hybridization of graphene fragment, which limits the nucleation and growth of onion-like nanoparticles. In addition, these particles have a chemically inert surface, which reduces the couple of dual interface via offering incommensurate and rolling contact (**Figure 10**).

5. Conclusions

FL-C:H films have been grown via PECVD and reactive magnetron sputtering methods. Such films with curved graphene dispersed in amorphous matrix, show elastic recovery (≥80), hardness (variation from 10 to 30 GPa) as well as low friction properties. Sometimes, FL-C:H films depict superlubricity within limited situation with the lowest coefficient value to 0.002. We believe that superlubricity of FL-C:H films benefits from the unique fullerene-like structure, which provide raw materials to grow onion-like nanoparticles during friction tests. In addition, these particles have a chemically inert surface, which reduces the couple of dual interface via offering incommensurate and rolling contact. But, further developing of the superlubricity properties of the FL-C:H films to wide adaptability is very important to broad practicability.

Acknowledgements

This work is supported by CAS "Light of West China" Program, Youth Innovation Promotion Association CAS (Grant no. 2017459), China Scholarship Council (File no. 201604910183) and the National Natural Science Foundation of China (Grant nos. 51205383, 51611530704 and 51661135022).

Author details

Bin Zhang[1,2,3]*, Kaixiong Gao[1,2], Yuanlie Yu[1,2] and Junyan Zhang[1,2]

*Address all correspondence to: bzhang@licp.cas.cn

1 R&D Center of Lubricating and Protecting Materials, Lanzhou Institute of Chemical Physics, Chinese Academy of Science, Lanzhou, Gansu, P.R. China

2 Key Laboratory of Solid Lubrication, Lanzhou Institute of Chemical Physics, Chinese Academy of Science, Lanzhou, Gansu, P.R. China

3 Lawrence Berkeley National Laboratory, Berkeley, CA, USA

References

[1] Hirano M, Shinjo K. Atomistic locking and friction. Physical Review B. 1990;**41**(17):11837. DOI: 10.1103/PhysRevB.41.11837

[2] Li J, Luo J. Advancements in superlubricity. Science China Technological Sciences. 2013;**56**(12):2877-2887. DOI: 10.1007/s11431-013-5387-y

[3] Berman D, Deshmukh SA, Sankaranarayanan SKRS, Erdemir A, Sumant AV. Macroscale superlubricity enabled by graphene nanoscroll formation. Science. 2015;**348**(6239):1118-1122. DOI: 10.1126/science.1262024

[4] Erdemir A. Design criteria for superlubricity in carbon films and related microstructures. Tribology International. 2004;**37**(7):577-583. DOI: 10.1016/j.triboint.2003.12.007

[5] Wang C, Yang S, Wang Q, Wang Z, Zhang J. Super-low friction and super-elastic hydrogenated carbon films originated from a unique fullerene-like nanostructure. Nanotechnology. 2008;**29**(22):225709. DOI: 10.1088/0957-4484/19/22/225709

[6] Martin JM, Pascal H, Donnet C, Le Mogne T, Loubet JL, Epicier T. Superlubricity of MoS2: Crystal orientation mechanisms. Surface and Coatings Technology. 1994;**68-69**: 427-432. DOI: 10.1016/0257-8972(94)90197-X

[7] Lantz MA, Wiesmann D, Gotsmann B. Dynamic superlubricity and the elimination of wear on the nanoscale. Nature Nanotechnology. 2009;**4**:586-591. DOI: 10.1038/nnano.2009.199

[8] Li H, Wood RJ, Rutland MW, Atkin R. An ionic liquid lubricant enables superlubricity to be "switched on" in situ using an electrical potential. Chemical Communications. 2014;**50**:4368-4370. DOI: 10.1039/C4CC00979G

[9] Li J, Zhang C, Ma L, Liu Y, Luo J. Superlubricity achieved with mixtures of acids and glycerol. Langmuir. 2013;**29**(1):271-275. DOI: 10.1021/la3046115

[10] Itamura N, Miura K, Sasak N. Simulation of scan-directional dependence of superlubricity of C60 molecular bearings and graphite. Japanese Journal of Applied Physics. 2009;**48**:060207. DOI: 10.1347-4065/48/6R/060207

[11] Hirano M, Shinjo K, Kaneko R, Murata Y. Observation of superlubricity by scanning tunneling microscopy. Physical Review Letters. 1997;**78**:1448. DOI: 10.1103/PhysRevLett.78.1448

[12] Donnet C, Mogne TL, Martin JM. Superlow friction of oxygen-free MoS2 coatings in ultrahigh vacuum. Surface and Coatings Technology. 1993;**62**(1-3):406-411. DOI: 10.1016/0257-8972(93)90275-S

[13] Dienwiebel M, Verhoeven GS, Pradeep N, Frenken JWM, Heimberg JA, Zandbergen HW. Superlubricity of graphite. Physical Review Letters. 2004;**92**:126101. DOI: 10.1103/PhysRevLett.92.126101

[14] Liu Z, Yang J, Grey F, Liu JZ, Liu Y, Wang Y, Yang Y, Cheng Y, Zheng Q. Observation of microscale superlubricity in graphite. Physical Review Letters. 2012;**108**:205503. DOI: 10.1103/PhysRevLett.108.205503

[15] Zhang R, Ning Z, Zhang Y, Zheng Q, Chen Q, Xie H, Zhang Q, Qian W, Wei F. Superlubricity in centimetres-long double-walled carbon nanotubes under ambient conditions. Nature Nanotechnology. 2013;**8**:912-916. DOI: 10.1038/nnano.2013.217

[16] Erdemir A, Eryilmaz OL, Fenske G. Synthesis of diamond like carbon films with superlow friction and wear properties. Journal of Vacuum Science & Technology A: Vacuum, Surfaces, and Films. 2000;**18**(4):582459. DOI: 10.1116/1.582459

[17] Andersson J, Erck RA, Erdemi A. Friction of diamond-like carbon films in different atmosphere. Wear. 2002;**51**:1070-1075. DOI: 10.1016/S0043-1648(03)00336-3

[18] Gong Z, Shi J, Zhang B, Zhang J. Graphene nano scrolls responding to superlow friction of amorphous carbon. Carbon. 2017;**116**:310-317. DOI: 10.1016/j.carbon.2017.01.106

[19] Erdemir A, Donnet C. Tribology of diamond-like carbon films: Recent progress and future prospects. Journal of Physics D: Applied Physics. 2006;**39**(18):R311-R327. DOI: 10.1088/0022-3727/39/18/R01

[20] Andersson J, Erck RA, Erdemir A. Frictional behavior of diamond like carbon films in vacuum and under varying water vapor pressure. Surface and Coatings Technology. 2003;**163**:535-540. DOI: 10.1016/S0257-8972(02)00617-5

[21] Wang X, Wang P, Zhang B, Yang S, Zhang J. The tribological properties of fullerene-like hydrogenated carbon (FL-C: H) film under different humidity conditions. Tribology Transactions. 2009;**52**(3):354-359. DOI: 10.1080/10402000802563125

[22] Zhou S, Wang L, Xue Q. Achieving low tribological moisture sensitivity by aC: Si: Al carbon-based coating. Tribology Letters. 2001;**43**:329-339. DOI: 10.1007/s11249-011-9814-6

[23] Shi J, Gong Z, Wang C, Zhang B, Zhang J. Tribological properties of hydrogenated amorphous carbon films in different atmospheres. Diamond and Related Materials. 2017;**77**:84-91. DOI: 10.1016/j.diamond.2017.06.005

[24] Wang Y, Zhang B, Gong Z, Gao K, Ou Y, Zhang J. The effect of a static magnetic field on the hydrogen bonding in water using frictional experiments. Journal of Molecular Structure. 2013;**1052**:102-104. DOI: 10.1016/j.molstruc.2013.08.021

[25] Gong Z, Jia X, Ma W, Zhang B, Zhang J. Hierarchical structure graphitic-like/MoS_2 film as superlubricity material. Applied Surface Science. 2017;**413**:381-386. DOI: 10.1016/j.apsusc.2017.04.057

[26] Gong Z, Shi J, Ma W, Zhang B, Zhang J. Engineering-scale superlubricity of the fingerprint-like carbon films based on high power pulsed plasma enhanced chemical vapor deposition. RSC Advances. 2016;**6**(116):115092-115100. DOI: 10.1039/C6RA24933G

[27] Wang P, Wang X, Zhang B, Liu W. Structural, mechanical and tribological behavior of fullerene-like carbon film. Thin Solid Films. 2010;**518**(21):5938-5943. DOI: 10.1016/j.tsf.2010.05.096

[28] Wang P, Wang X, Zhang B, Liu W. Formation of hydrogenated amorphous carbon films containing fullerene-like structures. Journal of Non-Crystalline Solids. 2009;**355**(34):1742-1746. DOI: 10.1016/j.jnoncrysol.2009.06.014

[29] Wang Y, Guo J, Gao K, Zhang B, Liang A, Zhang J. Understanding the ultra-low friction behavior of hydrogenated fullerene-like carbon films grown with different flow rates of hydrogen gas. Carbon. 2014;**77**:518-524. DOI: 10.1103/PhysRevB.75.205402

[30] Zhang L, Wang J, Zhang J, Zhang B. Increasing fluorine concentration to control the microstructure from fullerene-like to amorphous in carbon films. RSC Advances. 2016;**6**(26):21719-21724. DOI: 10.1039/C6RA00675B

[31] Qiang L, Zhang B, Gao K, Gong Z, Zhang J. Hydrophobic, mechanical, and tribological properties of fluorine incorporated hydrogenated fullerene-like carbon films. Friction. 2013;**1**(4):350-358. DOI: 10.1007/s40544-013-0031-1

[32] Wei L, Zhang B, Zhou Y, Qiang L, Zhang J. Ultra-low friction of fluorine-doped hydrogenated carbon film with curved graphitic structure. Surface and Interface Analysis. 2013;**45**(8):1233-1237. DOI: 10.1002/sia.5260

[33] Liu X, Yang J, Hao J, Zheng J, Gong Q, Liu W. A near-frictionless and extremely elastic hydrogenated amorphous carbon film with self-assembled dual nanostructure. Advanced Materials. 2012;**24**:4614-4617. DOI: 10.1002/adma.201200085

[34] Wang Q, Wang C, Wang Z, Zhang J. Fullerene nanostructure-induced excellent mechanical properties in hydrogenated amorphous carbon. Applied Physics Letters. 2007;**91**(14):141902. DOI: 10.1063/1.2794017

[35] Yan L, Zhao F, Li S, Hu Z, Zhao Y. Low-toxic and safe nanomaterials by surface-chemical design, carbon nanotubes, fullerenes, metallofullerenes, and graphenes. Nanoscale. 2011;**3**:362-382. DOI: 10.1039/C0NR00647E

[36] Zhang J, Zhang B, Xue Q, Wang Z. Ultra-elastic recovery and low friction of amorphous carbon films produced by a dispersion of multilayer graphene. Surface and Interface Analysis. 2012;**44**(2):162-165. DOI: 10.1002/sia.3787

[37] Liu DG, Tu JP, Gu CD, Hong CF, Chen R, Yang WS. Synthesis, structure and mechanical properties of fullerene-like carbon nitride films deposited by DC magnetron sputtering. Surface and Coatings Technology. 2010;**205**(7):2474-2482. DOI: 10.1016/j.surfcoat.2010.09.043

[38] Roy D, Chhowalla M, Wang H, Sano N, Alexandrou I, Clyne TW, Amaratunga GAJ. Characterisation of carbon nano-onions using Raman spectroscopy. Chemical Physics Letters. 2003;**373**(1-2):52-56. DOI: 10.1016/S0009-2614(03)00523-2

[39] Wang J, Cao Z, Pan F, Wang F, Liang A, Zhang J. Tuning of the microstructure, mechanical and tribological properties of a-C:H films by bias voltage of high frequency unipolar pulse. Applied Surface Science. 2015;**356**(30):695-700. DOI: 10.1016/j.apsusc.2015.08.091

[40] Robertson J. Mechanism of sp3 bond formation in the growth of diamond-like carbon. Diamond and Related Materials. 2005;**14**(3-7):942-948. DOI: 10.1016/j.diamond.2004.11.028

[41] Wang Y, Gao K, Shi J, Zhang J. Bond topography and nanostructure of hydrogenated fullerene-like carbon films: A comparative study. Chemical Physics Letters. 2016;**660**(1):160-163. DOI: 10.1016/j.cplett.2016.08.023

[42] Liu G, Zhou Y, Zhang B, Gao K, Qiang L, Zhang J. Monitoring the nanostructure of a hydrogenated fullerene-like film by pulse bias duty cycle. RSC Advances. 2016;**6**(64):59039-59044. DOI: 10.1016/j.cplett.2016.08.023

[43] Hellgren N, Johansson MP, Hjörvarsson B, Östblom M, Liedberg B, Hultman L, Sundgren J-E. Growth, structure, and mechanical properties of CNxHyCNxHy films deposited by dc magnetron sputtering in N2/Ar/H2 discharges. Journal of Vacuum Science & Technology A: Vacuum, Surfaces, and Films. 2000;**18**:2349. DOI: 10.1116/1.1286395

[44] Ruoff RS. Is C60 stiffer than diamond? Nature. 1991;**350**(6320):663-664. DOI: 10.1038/350663b0

[45] Brazhkin VV, Solozhenko VL, Bugakov VI, Dub SN, Kurakevych OO, Kondrin MV, Lyapin AG. Bulk nanostructured carbon phases prepared from C60: Approaching the 'ideal' hardness. Journal of Physics: Condensed Matter. 2007;**19**(23):236209. DOI: 10.1088/0953-8984/19/23/236209

[46] Wang Y, Guo J, Zhang J, Qin Y. Ultralow friction regime from the in situ production of a richer fullerene-like nanostructured carbon in sliding contact. RSC Advances. 2015;**5**:106476-106484. DOI: 10.1039/C5RA20892K

IntechOpen

IntechOpen

IntechOpen

IntechOpen